Biointerface Research in Applied Chemistry
Open-Access Journal (ISSN: 2069-5837)

Article
Volume 16, Issue 1, 2026, 36
https://doi.org/10.33263/BRIAC161.036

Formulation Development and Optimization of a Terbinafine Hydrochloride-Loaded Solid Lipid Nanoparticulate Gel for Enhanced Antifungal Efficacy Against *Candida albicans*

Renuka Patankar [1], Srinivas Bhairy [1,2], Rajashree Hirlekar [1,*]

[1] Department of Pharmaceutics, Vivekanand Education Society's College of Pharmacy, Affiliated to University of Mumbai, Mumbai 400074, Maharashtra, India
[2] Department of Formulations Research and Development, RelonChem-Bell's Son's Pharma UK Limited, Southport PR9 9AL, England, United Kingdom
* Correspondence: rajashree.hirlekar@ves.ac.in;

Received: 18.06.2025; Accepted: 15.11.2025; Published: 15.02.2026

Abstract: Terbinafine hydrochloride effectively treats superficial fungal infections, but oral use has side effects, and topical forms show poor penetration and short residence. Solid lipid nanoparticles (SLNs) enhance topical delivery by improving skin absorption, providing sustained drug release, and offering a stable, biocompatible carrier for more effective antifungal therapy. This study aimed to develop and optimize a terbinafine hydrochloride-loaded SLN gel to achieve minimal particle size and polydispersity index (PdI), high entrapment efficiency, and enhanced antifungal activity against *Candida albicans*. SLNs were prepared using a modified hot-melt emulsification followed by ultrasonication. Excipient selection was guided by solubility screening, and a 3^3 full-factorial design was used to optimize lipid content, surfactant concentration, and sonication duration. The optimized SLNs were incorporated into a Carbopol® 974P gel and characterized for particle size, PdI, zeta potential, entrapment efficiency, *in-vitro* drug release, antifungal efficacy, and stability. The optimized formulation produced SLNs with a particle size of 262 nm, a PDI of 0.3, and an entrapment efficiency of 96.88%. The SLN gel showed sustained drug release (85.3% over 24 h), stronger antifungal activity (28 mm inhibition zone) than a marketed cream (10 mm), and good stability for 60 d under International Council for Harmonisation of Technical Requirements for Pharmaceuticals for Human Use conditions. The developed SLN-based gel formulation of terbinafine hydrochloride demonstrated enhanced antifungal efficacy, controlled drug release, and excellent stability, making it a promising candidate for the topical treatment of fungal infections.

Keywords: terbinafine hydrochloride; solid lipid nanoparticles; hydrogel; antifungal activity.

1. Introduction

Fungal infections of the skin, scalp, and nails are commonly treated with oral or topical antifungals. Terbinafine hydrochloride, a widely used allylamine, demonstrates high efficacy and good tolerability via both routes [1]. Terbinafine hydrochloride accumulates in keratinized tissues, sustaining high local concentrations for weeks after treatment. Its potent antifungal activity, with low minimum inhibitory concentration (0.001–0.01 µg/mL) and minimum

fungicidal concentration (0.003-0.006 µg/mL) against dermatophytes, underpins its clinical utility in superficial mycoses [2]. Terbinafine hydrochloride is available orally and topically. Oral administration undergoes extensive first-pass metabolism (~40%) and high plasma protein binding, potentially requiring higher doses and increasing adverse effects. Topical delivery achieves high local concentrations with minimal systemic exposure [3,4]. Controlled drug delivery systems, especially nanocarriers, offer site-specific, time-controlled drug release, enhancing therapeutic efficacy and reducing systemic side effects [5,6]. SLNs are submicron colloidal carriers of physiological lipids stabilized in oil-in-water emulsions. They efficiently encapsulate drugs, enhance stability and permeability, and, as they are biocompatible and biodegradable, are safe for topical application [7]. SLNs enhance dermal drug delivery through their nanoscale size, promoting intimate contact with the stratum corneum and nail plate, improving permeation, and providing sustained release to maintain therapeutic levels while minimizing systemic exposure [8,9]. Numerous studies have developed SLN formulations of terbinafine hydrochloride for topical use. However, methods such as solvent injection raise safety concerns due to the potential for residual toxic organic solvents [4,10-12].

Additionally, alternative fabrication techniques such as high-pressure homogenization are associated with high production costs and complex processing requirements [13-15]. Furthermore, previously reported formulations often exhibited large particle sizes (exceeding 500 nm) [4], high polydispersity indices (0.4-0.6) [10], and variable or suboptimal drug entrapment efficiencies (ranging from 15 % to 90 %) [4], all of which can compromise therapeutic performance and formulation stability. This study aims to develop and characterize an optimized topical SLN formulation of terbinafine hydrochloride with minimal particle size and PdI, high entrapment efficiency, and a scalable, cost-effective manufacturing process to improve site-specific drug delivery.

2. Materials and Methods

2.1. Materials.

Terbinafine hydrochloride was obtained from Aarti Drugs Pvt. Ltd., India. Precirol® ATO 5 (glyceryl distearate) and Compritol® 888 ATO (glyceryl dibehenate) were kindly provided by Gattefossé, India. Glyceryl monostearate, stearic acid, and palmitic acid were procured from LobaChemie, India. Surfactants, including Kolliphor® PS 20 (Tween 20), Kolliphor® PS 60 (Tween 60), Kolliphor® PS 80 (Tween 80), Solutol® HS 15 (macrogol-15-hydroxystearate), Kolliphor® RH 40 (Polyoxyl 40 Hydrogenated Castor Oil), and Kolliphor® P 188 (Poloxamer 188) were sourced from BASF, India, while Tween™ 40 was obtained from Croda, India. Carbopol® 970P, 974P, and 980 (Carbomer polymer) were obtained from Lubrizol Corporation, India. Sabouraud Dextrose Agar and Nutrient Broth were purchased from HiMedia Laboratories Pvt. Ltd., India. All other chemicals used were of analytical grade.

2.2. Methods.

2.2.1. Formulation development of SLNs dispersion.

2.2.1.1. Screening of excipients.

Terbinafine hydrochloride solubility in lipids was assessed using a semi-quantitative method. Lipids were heated 5°C above their melting points, and the drug was added and mixed

using a vortex mixer (Remi Labs, India). The solubility limit was determined as the point at which no further drug dissolved. Surfactants were screened similarly, with heating applied only to solid components [16]. All the measurements are reported as mean (n = 3).

2.2.1.2. Fabrication of lipid nanoparticles.

In the modified hot melt emulsification method [17], terbinafine hydrochloride (100 mg) was dissolved in lipid heated 5-10°C above its melting point. Surfactant was added to the lipid phase, followed by hot aqueous phase addition and vortex mixing (Remi Labs, India). The resulting pre-emulsion was sonicated using a probe (3 mm horn, 30–40 % variac, 90 W; Oscar Ultrasonics Pvt Ltd, India) to reduce particle size.

2.2.1.3. Preliminary screening-formulation and process-related parameters.

Preliminary optimization was conducted using a one-factor-at-a-time methodology to evaluate the influence of lipid type and level, surfactant type and concentration, and sonication time on particle size and entrapment efficiency, while maintaining a constant terbinafine hydrochloride dose of 100 mg.

2.2.1.4. Optimization by design of experiment.

The effects of various parameters were statistically analyzed using one-way analysis of variance (ANOVA) in Design-Expert® v9.0.3 to evaluate both individual and combined contributions of formulation and process variables on the responses. A 3^3 full factorial design was used to optimize SLNs prepared via modified hot melt emulsification–ultrasonication. Effects of lipid concentration (A), surfactant concentration (B), and sonication time (C) on particle size and entrapment efficiency were evaluated at three levels (low, medium, and high). Experiments were performed in duplicate (n = 2), and model significance was established using ANOVA. Significance was defined as $p < 0.05$. Response criteria were set at ≤350 nm for particle size and 99 % for entrapment efficiency. Independent variables were defined as 'in range,' allowing any combination yielding responses within these limits. Polynomial coefficients were calculated to assess factor effects, and contour and 3D surface plots visualized factor–response relationships. Desirability and overlay plots guided the selection of the final optimized formulation, summarized in Table 1.

Table 1. Design of expert variables for optimization.

Levels	Factors			Response	
	X1 : LC	X2 : SC	X3 : ST	Y1	Y2
Low	800	250	6	PS (nm)	EE (%)
Medium	1000	300	8		
High	1200	350	10		

LC-Lipid concentration; SC-Surfactant concentration; ST-Sonication time; PS-Particle size; EE-Entrapment efficiency.

2.2.2. Characterization and evaluation of SLNs dispersion.

2.2.2.1. Appearance, particle size, size distribution, and zeta potential.

Appearance was assessed visually. Particle size and PdI of SLN dispersions were measured (n = 3) by dynamic light scattering (Malvern Zetasizer ZS90, UK) at 90° and 25°C,

maintaining scattering intensity of 100–500 kcps by appropriate dilution with double-distilled water [18]. Zeta potential was measured by laser doppler micro-electrophoresis [19,20].

2.2.2.2. Entrapment efficiency.

Entrapment efficiency of SLNs was determined indirectly by measuring unentrapped drug in the aqueous phase using saturated sodium chloride dilution [16]. Dispersions were mixed with sodium chloride solution, centrifuged (14,000 rpm, 30 min) (Remi Ltd., India), filtered (0.45 µm Millipore membrane, Merck Millipore, Germany), diluted with methanol, and analyzed at 283 nm using a UV-Vis Spectophotometer (Shimadzu 1800, Japan). Results are expressed as mean (n = 3). % entrapment efficiency was calculated using equation 1:

$$\text{Entrapment efficiency } (\%) = \frac{Wt - Wa}{Wt} X\ 100 \qquad (1)$$

Where W_t stands for the total amount of drug added to the system, W_a stands for the amount of drug quantified by the indirect method.

2.2.2.3. Fourier transform infrared (FTIR) study.

FTIR spectra of terbinafine hydrochloride and SLN dispersions were recorded (Shimadzu IRTracer-100, Japan) from 750-4000 cm^{-1} to assess drug entrapment. The absence or significant reduction of characteristic peaks of terbinafine hydrochloride in the IR spectra of the SLNs dispersion would confirm that the drug is effectively incorporated into the lipid carrier system.

2.2.3. Formulation development of SLNs gel.

The SLN dispersion exhibited low viscosity, limiting direct topical use. To improve stability, controlled release, and epidermal targeting, SLNs were incorporated into gels [21]. Various Carbopol® grades (0.5-2 % w/w) were dispersed in distilled water, stirred (100 rpm, 60 min), using a magnetic stirrer (Remi Labs, India) and neutralized with triethanolamine to pH 6.0.

2.2.4. Evaluation of SLNs gel.

2.2.4.1. Physical properties (appearance, pH, viscosity, extrudability, and spreadability).

Gel formulations were evaluated for appearance, consistency, and pH (Mettler Toledo SevenCompact™ S210). Viscosity was measured using a Brookfield viscometer (spindle S96, 10 rpm) (Anton Paar, Austria). Extrudability was assessed by the formation of uniform cylindrical extrudates, and spreadability was determined by gel diameter increase under a 500 g weight that was applied for 5 min (n = 3) [21].

2.2.4.2. Drug recovery.

Terbinafine hydrochloride SLN dispersions were diluted with methanol and bath sonicated (Oscar Ultrasonics Pvt Ltd, India) for 60 min for complete drug extraction, filtered through a 0.45 µm Millipore membrane (Merck Millipore, Germany), further diluted, and analyzed by UV-Vis spectrophotometer (Shimadzu 1800, Japan) (n = 3) [16]. Percentage recovery was calculated by equation 2.

$$\text{Recovery (\%)} = \frac{\text{Amount of terbinafine hydrochloride recovered}}{\text{Amount of terbinafine hydrochloride added}} \text{X } 100 \quad (2)$$

2.2.4.3. *In-vitro* drug release.

In-vitro drug release was performed using a Franz diffusion cell (Meditech Technologies India Pvt. Ltd, India) with a hydrated dialysis membrane (12–14 kDa, Sigma-Aldrich Co., India). Formulations including terbinafine dispersion, SLN gel, conventional gel, and marketed cream Daskil 1% (Novartis India Ltd., India) were loaded onto the membrane separately. Release medium was phosphate-buffered saline (pH 6.8) with 0.8 % Kolliphor® PS 80 at 37°C, 100 rpm. Samples (n = 3) were withdrawn at intervals, replaced with fresh medium, and analyzed at 283 nm using a UV-Visible spectrophotometer (Shimadzu 1800, Shimadzu, Japan). Data are presented as means and analyzed by ANOVA with Tukey's post-hoc test.

2.2.4.4. *In-vitro* antifungal activity.

In-vitro antifungal efficacy of the SLN gel and marketed terbinafine cream was evaluated against *Candida albicans* [21]. The inoculum was mixed with molten Sabouraud dextrose agar, poured into petri plates, and wells were loaded with test samples. After 24 h at 37 °C, zones of inhibition (mm) were measured (n = 4) and analyzed by one-way ANOVA ($p < 0.05$).

2.2.4.5. Real-time stability study.

Stability of terbinafine SLN gel was evaluated per ICH guidelines at 25 °C/60 % relative humidity (RH) and 40 °C/75 % RH [22]. Samples were analyzed at 0, 15, 30, and 60 d for appearance, extrudability, spreadability, viscosity, drug recovery, pH, and *in-vitro* release (n = 3). No significant changes were considered indicative of stability ($p > 0.05$).

3. Results and Discussion

3.1. Formulation development of SLNs dispersion.

3.1.1. Screening of excipients.

Terbinafine hydrochloride solubility in lipids decreased in the order, Glyceryl monostearate > Compritol® 888 ATO > Precirol® ATO 5 > Stearic acid > Palmitic acid. Due to their poor solubility, stearic acid and palmitic acid were excluded from further studies. Glyceryl monostearate combined with Compritol® 888 ATO showed the highest solubility. Among surfactants screened, Kolliphor® RH 40 and PS 80 provided maximal drug solubility (Figure 1).

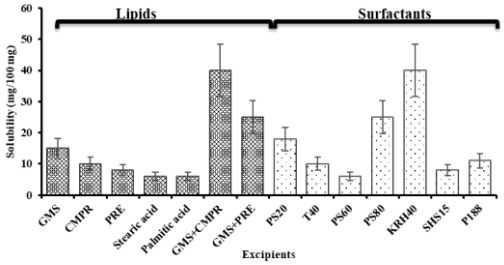

Figure 1. Apparent solubility of terbinafine hydrochloride in lipids and surfactants. [GMS-Glyceryl monostearate; CMPR- Compritol® 888 ATO; PRE- Precirol® ATO 5; PS20- Kolliphor® PS 20; T40- Tween™ 40; PS60- Kolliphor® PS 60; PS80- Kolliphor® PS 80; KRH40- Kolliphor® RH 40; SHS15- Solutol® HS 15; P188- Kolliphor® P 188].

3.1.2. Preliminary screening-formulation and process-related parameters.

3.1.2.1. Lipid variation in the formulation.

The effect of lipid type (800-1200 mg) was evaluated with Kolliphor® RH 40 as surfactant. Glyceryl monostearate produced moderately uniform particles (371.6–393.4 nm, PdI 0.389-0.448), while Compritol® 888 ATO yielded larger but slightly more uniform particles (446.76-519 nm, PdI 0.334-0.353). The combination of both lipids generated the smallest and most uniform particles (265.8-291 nm, PdI 0.112-0.240) and effectively minimized drug leakage, indicating improved stability and homogeneity of the SLN formulation.

3.1.2.2. Surfactant variation in the formulation.

Higher surfactant concentrations reduce the surface tension of molten lipid droplets, promoting their breakdown into smaller particles and preventing coalescence by stabilizing the droplet surface. With lipid composition (glyceryl monostearate and Compritol® 888 ATO) and lipid concentration (800 mg) fixed, different surfactants Kolliphor® PS 20, P 188, and RH 40 were tested at 250–350 mg with 10 min sonication. Kolliphor® PS 80 produced particle sizes of 265.8-299 nm (PdI 0.325-0.34), Kolliphor® P 188 yielded larger and less uniform particles (336.2-351.6 nm, PdI 0.374-0.420), whereas Kolliphor® RH 40 generated the smallest, most uniform particles (202-234 nm, PdI 0.270-0.300), demonstrating superior emulsification efficiency and stability. Formulations with Kolliphor® P 188 and PS 80 showed reduced physical stability after 3 days of storage.

3.1.2.3. Sonication time variation in the formulation.

Particle size and PdI decreased with increasing sonication time, as ultrasonication breaks coarse emulsion droplets into nanoscale particles. With lipid (glyceryl monostearate , Compritol® 888 ATO) and Kolliphor® RH 40 concentrations fixed, sonication times of 6, 8, and 10 min produced particle sizes of 291.2, 280.3, and 226 nm, with corresponding PdIs of 0.352, 0.304, and 0.211. 10 min of sonication yielded the smallest, most uniform particles. The optimal formulation combined the lipid mixture with Kolliphor® RH 40 and 10 min of sonication, producing 226 nm particles with a PdI of 0.211, indicating a stable, homogeneous system suitable for enhanced drug delivery.

3.1.3. Optimization by design of experiment.

Factorial designs are widely used for optimization, allowing the evaluation of multiple factors on observed responses. The drug amount was kept constant at 100 mg of terbinafine hydrochloride in all formulation trials.

3.1.3.1. Influence of the factors on the responses of terbinafine hydrochloride SLNs dispersion.

For response 1: Particle size

The particle size of the SLNs ranged from 210 to 362 nm, as observed in Table 2. Table 3 presents the ANOVA results generated by the software after inputting the particle size response data ($p < 0.05$).

The following parameters were obtained from the software for the particle size response: The model's F-value was found to be 2.93, indicating that the model was statistically

significant. There was only a 2.70 % probability that an F-value this large could result from random noise. The variables—surfactant concentration, sonication time, and lipid concentration—were identified as having a significant influence on this response. The predicted R^2 (Pred R^2) value of 0.3045 was in reasonable agreement with the adjusted R^2 (Adj R^2) value of 0.4004, with a difference of less than 0.2, suggesting good model reliability. Adequate precision, which measures the signal-to-noise ratio, was found to be 6.33. As a signal-to-noise ratio exceeding 4 is regarded as acceptable, the obtained value reflects a satisfactory signal strength. Consequently, the model is suitable for effective exploration of the design space.

Equation 3 was derived for particle size:

$$PS = 379.97 - 1.40A - 59.28B + 29.06C - 45.57AB + 66.98AC + 96.83BC + 20.49A^2 + 56.57B^2 - 102.63C^2 \quad (3)$$

Where PS-Particle size; A-Surfactant concentration; B-Sonication time; C-Lipid concentration

Table 2. Responses observed in a 3^3 factorial design for terbinafine hydrochloride SLNs dispersion.

Runs	SC (mg)	ST (min)	LC (mg)	PS (nm)	EE (%)
1	250	6	800	291.5	95.8
2	300	6	800	280.3	99.3
3	350	6	800	235.3	99.7
4	250	8	800	291	97.4
5	300	8	800	267.7	99.3
6	350	8	800	210.7	98.6
7	250	10	800	346.6	95.9
8	300	10	800	275.6	99.136
9	350	10	800	262	96.88
10	250	6	1000	235.6	98.5
11	300	6	1000	287	97.95
12	350	6	1000	282.7	95.8
13	250	8	1000	293	97.7
14	300	8	1000	255.6	96.21
15	350	8	1000	362.7	98.8
16	250	10	1000	285.3	97.34
17	300	10	1000	219.2	95.93
18	350	10	1000	266.5	96.21
19	250	6	1200	301	99.46
20	300	6	800	226.3	97.33
21	350	6	1200	318.4	98.29
22	250	8	1200	213.3	95.7
23	300	8	1200	270	91.66
24	350	8	1200	233	98.62
25	250	10	1200	200.3	96.26
26	300	10	1200	247.9	99.68
27	350	10	1200	227	99.56

SC-Surfactant concentration; ST-Sonication time; LC-Lipid concentration; PS-Particle size; EE-Entrapment efficiency.

The model indicated that both surfactant concentration (factor A) and sonication time (factor B) negatively affected particle size, with higher levels reducing particle size. The coefficient for sonication time (59.28) was much larger than for surfactant concentration (1.40), indicating sonication time has a greater impact on particle size. Ultrasonication reduces coarse emulsion droplets to the nanoscale by generating shear stress, breaking larger droplets formed during emulsification. Higher surfactant concentrations further lower surface tension, facilitating droplet breakdown. Thus, both sonication and surfactant concentration significantly influence particle size. Contour and 3D response surface plots illustrated the relationship

between factors and responses. These plots visualize changes in response as two factors vary simultaneously and highlight deviations of the actual design points from the predicted values, indicating the model's predictive accuracy. Figures 2a, 2b, and 2c show contour plots indicating that particle size decreased with increasing surfactant concentration, sonication time, and lipid concentration. Similar trends are observed in the corresponding 3D response surface plots (Figures 2d, 2e, and 2f).

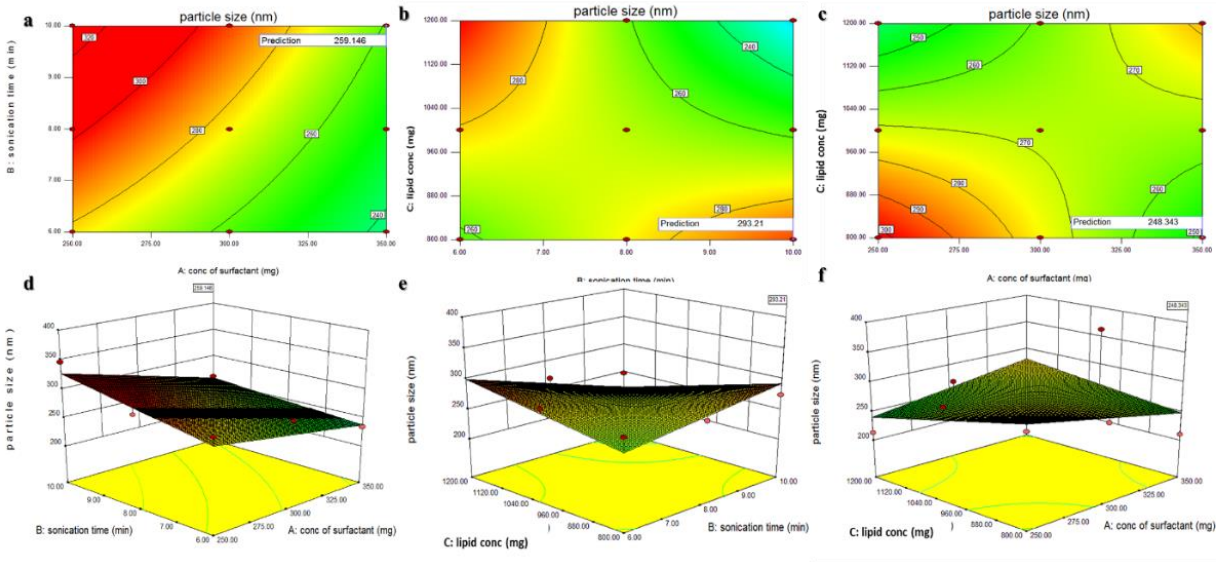

Figure 2. Contour plot **(a**, **b**, **c)**; 3D surface plot **(d**, **e,f)** for response particle size.

For response 2: Entrapment efficiency

The entrapment efficiency of terbinafine hydrochloride SLN dispersion ranged from 91.66% to 99.68%, as observed from the data presented in Table 2. Table 3 shows the ANOVA results generated by the software after entering the entrapment efficiency response data.

Table 3. Results of ANOVA for the response particle size and response entrapment efficiency.

Source	Response particle size			Response entrapment efficiency		
	F value	p-value Prob> F		F value	p-value Prob> F	
Model	2.93	0.0270	significant	0.56	0.8071	Not significant
A-SC	2.622E-003	0.9598		0.68	0.4202	
B-ST	5.70	0.0446		0.41	0.5329	
C-LC	1.13	0.3027		0.33	0.5720	
AB	1.85	0.1913		1.55	0.2298	
BC	5.00	0.0617		1.50	0.2374	
AC	8.36	0.0101		0.40	0.5355	

SC-Surfactant concentration; ST-Sonication time; LC-Lipid concentration.

The following parameters were obtained from the software for the response entrapment efficiency: the model's F-value was 0.56, indicating the model was not statistically significant. There was an 80.71 % probability that an F-value this large could result from random noise. he variables—surfactant concentration, sonication time, and lipid concentration—were found to have no significant effect on this response. The predicted R^2 (Pred R^2) value of 0.9644 was not in reasonable agreement with the adjusted R^2 (Adj R^2) value of 0.1733, indicating poor model reliability. Adequate precision, which measures the signal-to-noise ratio, was calculated to be 3.28. Since a ratio greater than 4 is considered desirable, this value indicates an inadequate signal. Therefore, the model cannot be reliably used to navigate the design space.

Equation 4 derived for entrapment efficiency:

$$EE = 97.23 - 0.80A + 0.62B + 0.65C + 1.46AB + 1.48AC - 0.75BC - 0.60A^2 - 0.18B^2 - 0.46C^2 \quad (4)$$

where, EE-Entrapment efficiency; A-Surfactant concentration; B-Sonication time; C-Lipid concentration

Entrapment efficiency was found to be significantly influenced by both lipid concentration and sonication time. As sonication time and lipid concentration increase, the entrapment efficiency also increases. The contour and 3D response surface plots also indicated that entrapment efficiency increases with increasing sonication time and lipid concentration. Surfactant concentration, however, did not have a significant effect on entrapment efficiency. Figures 3a, 3b, and 3c illustrate the contour plots, while Figures 3d, 3e, and 3f present the corresponding 3D response surface plots for the entrapment efficiency response.

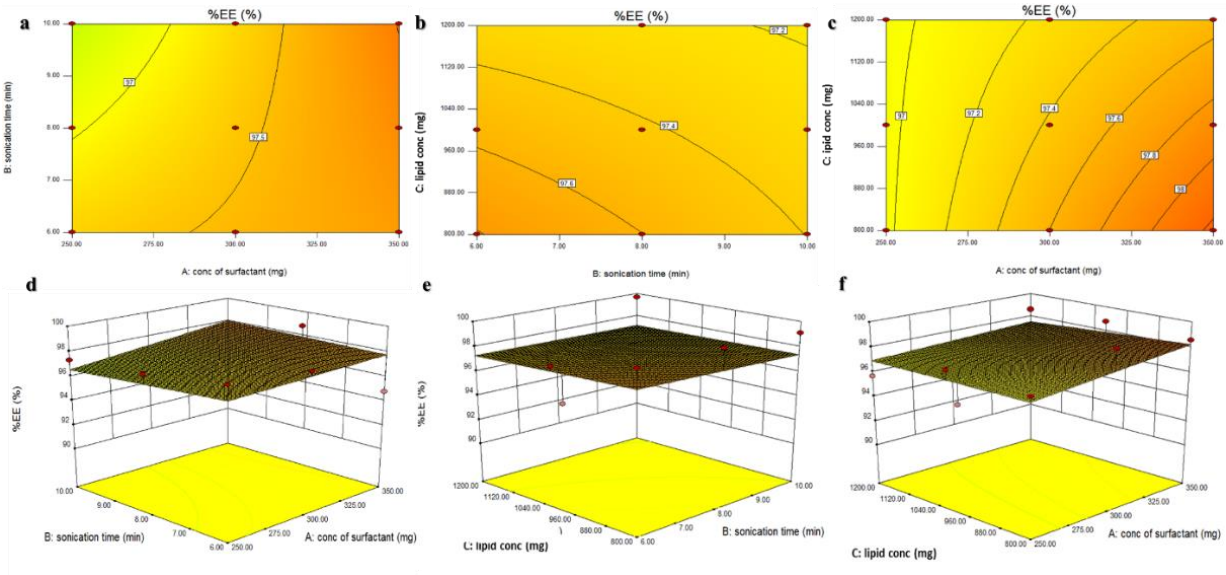

Figure 3. Contour plot **(a,b,c)**; 3D surface plot **(d,e, f)** for response entrapment efficiency.

Figures 4a and 4b show the correlation graphs of predicted versus actual values for the responses particle size and entrapment efficiency, respectively.

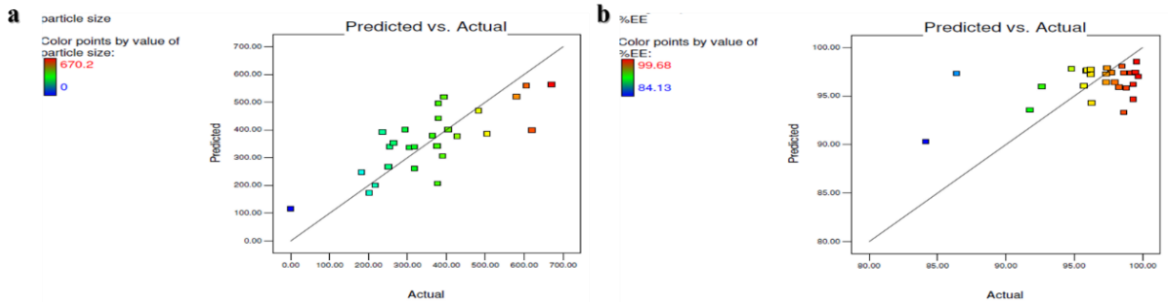

Figure 4. Correlation graphs of predicted versus actual values for the responses: **(a)** particle size; **(b)** entrapment efficiency.

The desirability plot (Figure 5a) identifies the region (working space) where any formulation prepared is expected to yield response values within the desired range. The overlay plot (Figure 5b) considers all target response values simultaneously and highlights the area that meets all criteria by combining the factors. In the desirability plot, it is evident that formulations prepared at high levels of both surfactant concentration and sonication time achieve the highest desirability value of 1. The red-colored area represents the working range for the optimized

formulation. Similarly, the yellow-colored region in the overlay plot indicates the suitable working region for the optimized formulation.

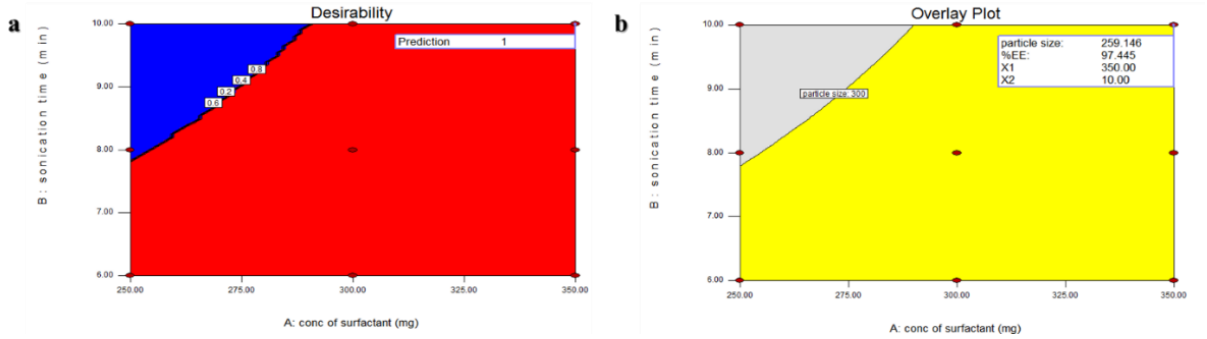

Figure 5. (a) The desirability plot; **(b)** the overlay plot for the terbinafine hydrochloride SLNs dispersion.

3.1.3.2. Optimized SLNs dispersion formulation.

From the overlay plot in Figure 5b, it is evident that at the highest surfactant concentration and sonication time, all responses fall within the desired limits. Hence, this formulation was selected as the optimized batch of terbinafine hydrochloride SLNs. Specifically, a surfactant concentration of 350 mg and a sonication time of 10 min were used. The optimized SLNs formulation comprised glyceryl monostearate and Compritol® 888 ATO (800 mg), Kolliphor® RH 40 (350 mg), and terbinafine hydrochloride (100 mg).

3.2. Characterization and evaluation of SLNs dispersion.

3.2.1. Appearance, particle size, size distribution, and zeta potential.

The terbinafine hydrochloride SLNs dispersion appeared as a white, uniform mixture with no phase separation or lipid aggregation. Particle size was 262 nm with a PdI of 0.300 (Figure 6a), indicating a fairly uniform distribution. The zeta potential was 7.75 mV (Figure 6b), suggesting moderate stability, as high positive or negative potentials prevent particle aggregation through mutual repulsion. Positively charged particles can adhere to negatively charged biological surfaces, and vice versa. Kolliphor® RH 40 served as the stabilizer, providing steric repulsion via hydrophilic polyoxyethylene chains that form a protective shell around nanoparticles, thereby enhancing colloidal stability.

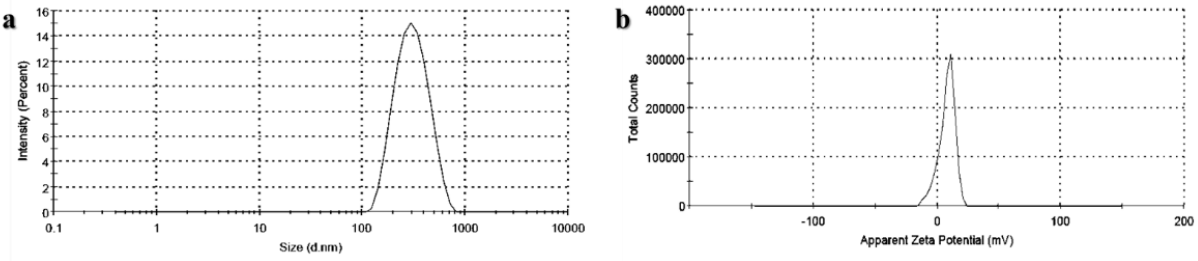

Figure 6. (a) Particle size; **(b)** zeta potential of terbinafine hydrochloride SLNs dispersion.

3.2.2. Entrapment efficiency.

The SLNs showed an entrapment efficiency of 96.88 %, indicating effective drug incorporation. High entrapment was essential due to the drug's poor aqueous solubility and susceptibility to degradation. Entrapment efficiency affects release characteristics and depends on formulation composition and production methods. Drug solubility in the lipid matrix was a key factor, and increasing surfactant concentration enhanced encapsulation by improving

solubilization and stabilization. High entrapment protects the drug, reduces degradation, and supports sustained release, thereby improving bioavailability.

3.2.3. Fourier transform infrared (FTIR) study.

FTIR spectra confirmed the entrapment of terbinafine hydrochloride within the SLNs by comparing the peaks of the pure drug (Figure 7a), excipients Compritol® 888 ATO (Figure 7b), glyceryl monostearate (Figure 7c), Kolliphor® RH 40 (Figure 7d), and the final SLNs dispersion (Figure 7e). In the pure drug, distinct peaks were observed for N–H stretching (~3296 cm^{-1}), aromatic C=C (~1605 cm^{-1}), and C–N (1244–1035 cm^{-1}). In the SLN's spectrum, these peaks were weakened, shifted, or absent, indicating strong molecular interactions and changes in the microenvironment due to encapsulation. The spectrum was dominated by broad lipid and surfactant peaks, including C–H and ester C=O from Compritol® 888 ATO and glyceryl monostearate, and ether C–O from Kolliphor® RH 40, showing the drug's embedding within the lipid matrix. The loss or reduction of specific terbinafine peaks confirms that the drug is entrapped in the lipid core, likely via hydrogen bonding or van der Waals interactions, demonstrating successful molecular-level loading.

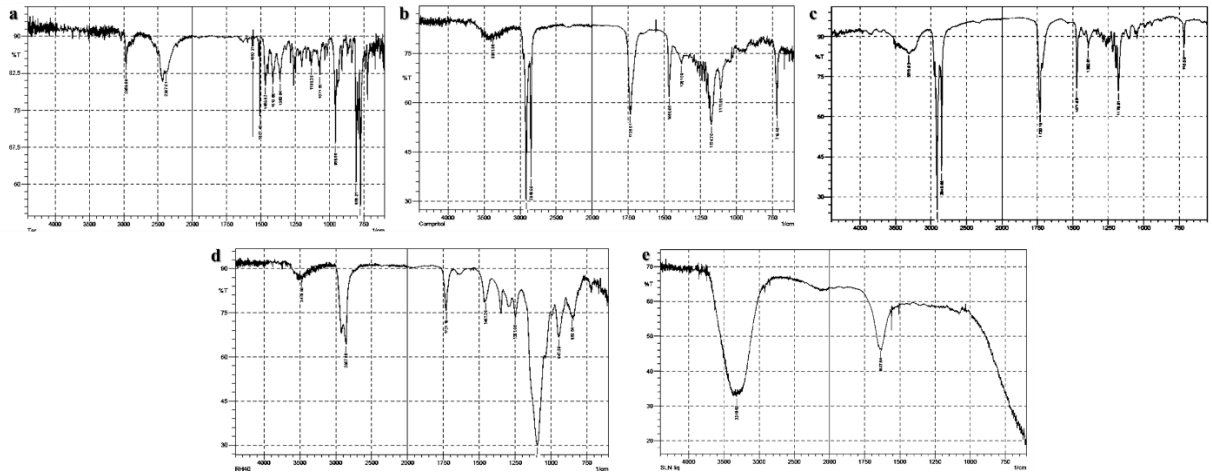

Figure 7. FTIR spectra of **(a)** terbinafine hydrochloride; **(b)** Compritol® 888 ATO; **(c)** glyceryl monostearate; **(d)** Kolliphor® RH 40; **(e)** terbinafine hydrochloride SLNs dispersion.

3.3. Formulation development of SLNs gel.

The SLNs dispersion had low viscosity, making it unsuitable for direct topical use. Hydrogels offer controlled release and better epidermal targeting. Among gelling agents tested, Carbopol® 970P produced a low-viscosity gel, while Carbopol® 980 was gritty. Therefore, 1 % Carbopol® 974P was chosen for the optimized formulation.

3.4. Evaluation of SLNs gel.

3.4.1. Physical properties (Appearance, pH, viscosity, extrudability, and spreadability).

The terbinafine hydrochloride SLNs gel was white and translucent, with a smooth consistency, good extrudability, and satisfactory spreadability. The viscosity of the gel was found to be 71,640 cPs, with an average pH of 6.0.

3.4.2. Drug recovery.

The assay of terbinafine hydrochloride in the SLN formulation was found to be 103.77%, indicating accurate drug content and uniform distribution within the formulation.

3.4.3. *In-vitro* drug release.

The drug release profile (Figure 8) showed that four terbinafine hydrochloride formulations released the drug over 24 h. The marketed cream showed the fastest, near-complete release (105.6 %), indicating immediate release. The drug dispersion also released rapidly (100.4 %) due to surfactant-mediated solubilization. The conventional gel released 97.6 % more gradually, suggesting moderate sustained release. In contrast, the SLNs gel exhibited an initial burst followed by slower, sustained release, reaching 85.3 % at 24 h. The biphasic pattern reflects a surface-adsorbed drug causing the initial release, while a lipid-encapsulated drug contributes to prolonged release. This dual profile is advantageous for antifungal therapy, enabling rapid reduction of fungal load and maintenance of therapeutic levels. Statistical analysis confirmed significant differences ($p < 0.05$) between the SLN gel and marketed cream, highlighting the sustained-release advantage of the SLN formulation.

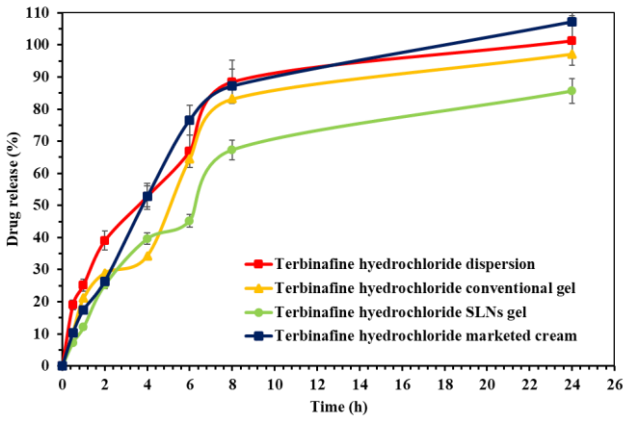

Figure 8. *In-vitro* drug release of terbinafine hydrochloride-dispersion, conventional gel, SLNs gel, and marketed cream.

3.4.4. *In-vitro* antifungal activity.

In vitro antifungal studies against Candida albicans on Sabouraud dextrose agar showed that the SLN dispersion and the SLN gel produced larger zones of inhibition (21 and 28 mm, respectively) than the marketed cream (10 mm) at 1 % concentration ($p < 0.001$). The enhanced activity is likely due to the nanoscale size of the drug in SLNs, which promotes faster diffusion, and to the hydrophilic polymers in the gel, which may improve drug permeation through the agar, contributing to superior antifungal performance.

3.4.5. Real-time stability study.

The stability study results indicated that the SLNs gel formulation remained stable over a period of 60 d, with no significant changes ($p > 0.05$) in appearance, extrudability, spreadability, viscosity (in the range of 71370-73565 cPs), drug recovery (in the range of 101.21-103.77 %), pH (in the range of 6.0-6.2). The *in-vitro* drug release profile (Figure 9) showed a consistent release pattern, supporting the formulation's stability.

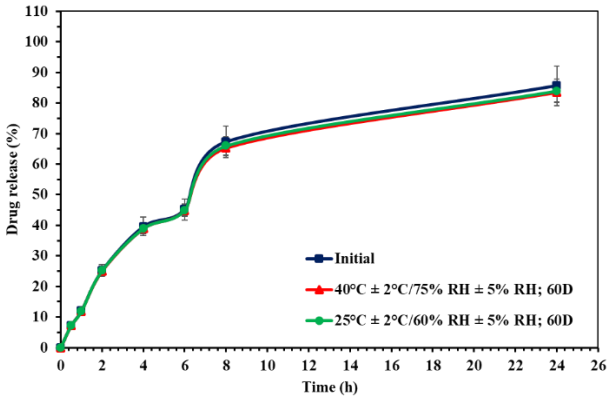

Figure 9. *In-vitro* drug release of terbinafine hydrochloride SLNs dispersion on real-time stability.

This study reports the successful development and optimization of an SLN-based terbinafine hydrochloride hydrogel for enhanced topical antifungal therapy against *Candida albicans*. Glyceryl monostearate is a monoglyceride, while Compritol® 888 ATO and Precirol® ATO 5 contain mixed fatty acid esters, exhibiting fewer polymorphic transitions and higher drug-loading capacity. Stearic and palmitic acids show lower loading due to their highly crystalline structures. Lipid crystal structure, influenced by processing conditions, can promote aggregation in NLCs. In lipid nanoparticles, stability is maintained by surfactants, which enhance lipid packing and prevent aggregation. Smaller, uniform particles further improve colloidal stability by reducing sedimentation and aggregation [18,23]. SLNs were prepared using a modified hot melt emulsification–ultrasonication method, eliminating organic solvents and enabling safe, scalable production. Key variables were optimized using a 3^3 full factorial design to achieve minimal particle size, low PdI, and high entrapment efficiency. Glyceryl monostearate and Compritol® 888 ATO were selected for their superior solubilization of terbinafine hydrochloride and their synergistic ability to reduce particle size and improve stability. Among the tested surfactants, Kolliphor® RH 40 produced the most uniform and stable nanoparticles through steric stabilization mediated by its polyoxyethylene chains. Sonication time strongly affected particle size, with durations up to 10 min efficiently reducing droplet size through cavitational forces. As reported by Sanming Li *et al*., appropriate surfactants promote electrostatic repulsion, preventing aggregation and improving colloidal stability. In contrast, inadequate surfactant coverage allows van der Waals–driven flocculation and potential gel formation due to changes in particle surface properties [24]. Design-Expert® analysis showed that sonication time and surfactant concentration were the primary determinants of particle size, with ANOVA confirming a significant predictive model ($p < 0.05$. Entrapment efficiency ranged from 91.66 % to 99.68 %, with the optimized batch achieving 96.88 %, indicating effective drug incorporation. The optimized formulation containing terbinafine hydrochloride (100 mg), lipid blend (800 mg), Kolliphor® RH 40 (350 mg), and 10 min of sonication produced nanoparticles with a diameter of 262 nm and a PdI of 0.3, indicating a uniform dispersion suitable for topical use. Particle size and PdI decreased with sonication due to cavitation, where bubble collapse generates shear forces that reduce droplets to the nanoscale. Excessive sonication, however, caused collisions and aggregation, increasing particle size. Thus, intermediate sonication times were optimal for achieving uniform nanoparticles [25]. The zeta potential (+7.75 mV) indicated moderate electrostatic and steric stability, minimizing the likelihood of particle aggregation. FTIR analysis confirmed drug encapsulation, as characteristic terbinafine hydrochloride peaks were markedly

diminished or absent in the SLN spectra, suggesting effective entrapment and possible molecular interactions with the lipid matrix. These findings align with previously reported literature [10]. Because the SLN dispersion exhibited low viscosity and unsuitable rheology for topical use, it was incorporated into a hydrogel containing 1 % Carbopol® 974P, which provided optimal consistency, spreadability, and compatibility without grittiness or phase separation. The resulting SLN gel was white, translucent, and smooth, with an acceptable pH (~6.0) [10], high viscosity (~71,640 cPs), and good spreadability and extrudability, supporting patient compliance. Drug content was high (103.77 %), indicating uniform distribution and minimal degradation. *In vitro* release studies using Franz diffusion cells showed a biphasic profile, an initial burst followed by sustained release with 85.3 % cumulative release over 24 h. This aligns with the mechanism described by Gardouh *et al*., where diffusion proceeds through water penetration, matrix swelling, lipid transition to a rubbery state, and subsequent drug release from the swollen matrix [26]. This release pattern is advantageous for antifungal therapy, as the initial burst rapidly reduces fungal load while the sustained phase maintains drug levels at the infection site, potentially lowering dosing frequency and improving adherence. Unlike the marketed cream, which released over 100 % of the drug within 24 h, the SLN gel provided controlled, prolonged release, demonstrating the superiority of the nanocarrier system. Enhanced antifungal efficacy was confirmed in vitro, with the SLN gel producing a significantly larger inhibition zone (28 mm vs. 10 mm), reflecting improved diffusion of the nanosized particles. This increased activity likely stems from better drug penetration through the fungal biofilm and agar matrix facilitated by the SLN hydrogel system. The study was limited to *in vitro* evaluations without *in vivo* or clinical testing, restricting insights into pharmacokinetics, skin permeation depth, and therapeutic performance under physiological conditions. Stability testing was short-term, which may not reflect long-term behavior. Future research should include *ex vivo* and *in vivo* studies to confirm skin retention, bioavailability, and safety, alongside extended stability assessments and scalability validation.

4. Conclusions

This study developed an optimized terbinafine hydrochloride SLN-based gel for improved topical antifungal therapy. SLNs prepared by hot melt emulsification–ultrasonication using glyceryl monostearate, Compritol® 888 ATO, and Kolliphor® RH 40 achieved 262 nm size, PdI 0.3, and 96.88 % entrapment. Incorporation into a 1 % Carbopol® 974P gel produced suitable rheology, pH, and uniform drug content. The gel showed biphasic release and significantly greater antifungal activity (28 mm) than the marketed cream (10 mm). FTIR confirmed drug encapsulation, and real-time stability data demonstrated the formulation's stability over 60 days.

Author Contributions

Conceptualization, R.H.; methodology, R.P.; software, R.P. and S.B.; validation, R.H.; formal analysis, R.P.; investigation, R.P.; resources, R.H.; data curation, R.H.; writing—original draft preparation, S.B.; writing—review and editing, R.H. and S.B.; visualization, S.B.; supervision, R.H.; project administration, R.H.; funding acquisition, R.H. All authors have read and agreed to the published version of the manuscript.

Institutional Review Board Statement

Not applicable.

Informed Consent Statement

Not applicable.

Data Availability Statement

Data supporting the findings of this study are available upon reasonable request from the corresponding author.

Funding

The research received no external funding.

Acknowledgments

Not applicable.

Conflicts of Interest

The authors declare no conflict of interest.

References

1. Trombino, S.; Mellace, S.; Cassano, R. Solid Lipid Nanoparticles for Antifungal Drugs Delivery for Topical Applications. *Ther. Deliv.* **2016**, *7*, 639–647, https://doi.org/10.4155/tde-2016-0040.
2. Tanrıverdi, S.T.; Özer, Ö. Novel topical formulations of Terbinafine-HCl for treatment of onychomycosis. *Eur. J. Pharm. Sci.* **2013**, *48*, 628-636, https://doi.org/10.1016/j.ejps.2012.12.014.
3. Darkes, M.J.M.; Scott, L.J.; Goa, K.L. Terbinafine. *Am. J. Clin. Dermatol.* **2003**, *4*, 39-65, https://doi.org/10.2165/00128071-200304010-00005.
4. Vaghasiya, H.; Kumar, A.; Sawant, K. Development of solid lipid nanoparticles based controlled release system for topical delivery of terbinafine hydrochloride. *Eur. J. Pharm. Sci.* **2013**, *49*, 311-322, https://doi.org/10.1016/j.ejps.2013.03.013.
5. Din, F.U.; Aman, W.; Ullah, I.; Qureshi, O.S.; Mustapha, O.; Shafique, S.; Zeb, A. Effective use of nanocarriers as drug delivery systems for the treatment of selected tumors. *Int. J. Nanomed.* **2017**, *12*, 7291–7309, https://doi.org/10.2147/IJN.S146315.
6. Patra, J.K.; Das, G.; Fraceto, L.F.; Campos, E.V.R.; Rodriguez-Torres, M.d.P.; Acosta-Torres, L.S.; Diaz-Torres, L.A.; Grillo, R.; Swamy, M.K.; Sharma, S.; Habtemariam, S.; Shin, H.-S. Nano based drug delivery systems: recent developments and future prospects. *J. Nanobiotechnol.* **2018**, *16*, 71, https://doi.org/10.1186/s12951-018-0392-8.
7. Souto, E.B.; Müller, R.H. The use of SLN and NLC as topical particulate carriers for imidazole antifungal agents. *Pharmazie* **2006**, *61*, 431–437.
8. Lv, Q.; Yu, A.; Xi, Y.; Li, H.; Song, Z.; Cui, J.; Cao, F.; Zhai, G. Development and evaluation of penciclovir-loaded solid lipid nanoparticles for topical delivery. *Int. J. Pharm.* **2009**, *372*, 191-198, https://doi.org/10.1016/j.ijpharm.2009.01.014.
9. Liu, J.; Hu, W.; Chen, H.; Ni, Q.; Xu, H.; Yang, X. Isotretinoin-loaded solid lipid nanoparticles with skin targeting for topical delivery. *Int. J. Pharm.* **2007**, *328*, 191-195, https://doi.org/10.1016/j.ijpharm.2006.08.007.
10. Abobakr, F.E.; Fayez, S.M.; Elwazzan, V.S.; Sakran, W. Effect of Different Nail Penetration Enhancers in Solid Lipid Nanoparticles Containing Terbinafine Hydrochloride for Treatment of Onychomycosis. *AAPS PharmSciTech* **2021**, *22*, 33, https://doi.org/10.1208/s12249-020-01893-9.

11. Abobakr, F.E.; Fayez, S.M.; Elwazzan, V.S.; Sakran, W. Formulation and optimization of terbinafine hcl solid lipid nanoparticles for topical antifungal activity. *Int. J. Pharm. Pharm. Sci*. **2019**, *11*, 16-25, https://doi.org/10.22159/ijpps.2019v11i12.35560.
12. Kumar, N.R.; Syed, S.M.; Sowmya, T. Development of formulation and evaluation of topical micro emulsion gel loaded with terbinafine HCL micro emulsion. *World J. Biol. Pharm. Health Sci*. **2024**, *19*, 074–089, https://doi.org/10.30574/wjbphs.2024.19.2.0483.
13. Tiwari, S.; Mistry, P.; Patel, V. SLNs Based on Co-Processed Lipids for Topical Delivery of Terbinafine Hydrochloride. *J. Pharm. Drug Dev*. **2014**, *2*, 404, https://doi.org/10.15744/2348-9782.1.604.
14. Chen, Y.-C.; Liu, D.-Z.; Liu, J.-J.; Chang, T.-W.; Ho, H.-O.; Sheu, M.-T. Development of terbinafine solid lipid nanoparticles as a topical delivery system. *Int. J. Nanomed.* **2012**, *7*, 4409–4418, https://doi.org/10.2147/IJN.S33682.
15. Rarokar, N.R.; Menghani, S.S.; Kerzare, D.R.; Khedekar, P.B.; Bharne, A.P.; Alamri, A.S.; Alsanie, W.F.; Alhomrani, M.; Sreeharsha, N.; Asdaq, S.M.B. Preparation of Terbinafin-Encapsulated Solid Lipid Nanoparticles Containing Antifungal Carbopol® Hydrogel with Improved Efficacy: In Vitro, Ex Vivo and In Vivo Study. *Pharmaceutics* **2022**, *14*, 1393, https://doi.org/10.3390/pharmaceutics14071393.
16. Hirlekar, R.; Bhairy, S.; Momin, A. Formulation Development and Evaluation of Dry Adsorbed Nanoparticles of Curcumin and Piperine Dual Drug Loaded Nanostructured Lipid Carriers. *Int. J. Pharm. Sci. Nanotechnol.* **2023**, *16*, 6844-6864, https://doi.org/10.37285/ijpsn.2023.16.4.2.
17. Hirlekar, R.; Momin, A.; Bhairy, S. Formulation development, in-vitro and ex-vivo evaluation of dry adsorbed solid lipid nanoparticles: an approach of overcoming olanzapine drawbacks. *Eur. Pharm. J.* **2024**, *71*, 1-15, https://doi.org/10.2478/afpuc-2024-0004.
18. Hirlekar, R.; Patil, E.; Bhairy, S. Solid nanostructured lipid carriers loaded with silymarin for oral delivery: Formulation development and evaluation. *Curr. Trends Pharm. Pharm. Chem*. **2021**, *3*, 56-67, https://doi.org/10.18231/j.ctppc.2021.014.
19. Patel, S.; Shah, J.; Bhairy, S.; Hirlekar, R. Development of Curcumin loaded Nanostructured Lipid Carriers: Preparation, Characterization and In-vitro Evaluation of Anti-cancer Activity Against A-549 Human Lung Cancer Cell Line. *J. Cancer Tumor Int.* **2021**, *11*, 66-88, https://doi.org/10.9734/jcti/2021/v11i430162.
20. Shah, J.; Patel, S.; Bhairy, S.; Hirlekar, R. Formulation optimization, characterization and in vitro anti-cancer activity of curcumin loaded nanostructured lipid carriers. *Int. J. Curr. Pharm. Res.* **2022**, *14*, 31-43, https://doi.org/10.22159/Ijcpr.2022v14i1.44110.
21. Gupta, S.B.; Bhairy, S.R.; Hirlekar, R.S. Formulation development, characterization and assessment of *In-Vitro* antifungal efficacy against *Candida albicans* of diallyl disulphide liposomal gel using 3^2 factorial design. *J. Drug Deliv. Ther*. **2019**, *9*, 105-117, https://doi.org/10.22270/jddt.v9i2.2522.
22. Ich harmonised tripartite guideline. stability testing of new drug substances and products Q1A(R2). Available online: https://database.ich.org/sites/default/files/Q1A%28R2%29%20Guideline.pdf (accessed on 17 January **2025**).
23. Mistry, K.R.; Sarker, D.K. SLNs can Serve as the New Brachytherapy Seed: Determining Influence of Surfactants on Particle Size of Solid Lipid Microparticles and Development of Hydrophobised Copper Nanoparticles for Potential Insertion. *J. Chem. Eng. Process Technol.* **2016**, *7*, 1000302, https://doi.org/10.4172/2157-7048.1000302.
24. Han, F.; Li, S.; Yin, R.; Liu, H.; Xu, L. Effect of surfactants on the formation and characterization of a new type of colloidal drug delivery system: Nanostructured lipid carriers. *Colloids Surf. A Physicochem. Eng. Asp.* **2008**, *315*, 210–216, https://doi.org/10.1016/j.colsurfa.2007.08.005.
25. Siddiqui, A.; Alayoubi, A.; El-Malah, Y.; Nazzal, S. Modeling the effect of sonication parameters on size and dispersion temperature of solid lipid nanoparticles (SLNs) by response surface methodology (RSM). *Pharm. Dev. Technol.* **2014**, *19*, 342–346, https://doi.org/10.3109/10837450.2013.784336.
26. Gardouh, A.R.; Gad, S.; Ghonaim, H.M.; Ghorab, M.M. Design and Characterization of Glyceryl Monostearate Solid Lipid Nanoparticles Prepared by High Shear Homogenization. *J. Pharm. Res. Int.* **2013**, *3*, 326–346, https://doi.org/10.9734/BJPR/2014/2770.

Publisher's Note & Disclaimer